GPS AS A STRUCTURAL DEFORMATION SENSOR

E. Harrison Teague*, Jonathan P. How†, London G. Lawson‡, Bradford W. Parkinson§
Department of Aeronautics and Astronautics, Stanford University, Stanford CA

Abstract

A new method of sensing the vibrational motions of a flexible structure by measuring the difference in GPS (global positioning system) carrier phase at separate antennas on the structure is presented. Differential carrier phase measurements have been recently used to determine the attitude of rigid bodies such as aircraft and spacecraft, and for aircraft landing with ground based GPS pseudolites. This technology is still rapidly developing and has often proven to be a powerful, low cost alternative to traditional sensing methods. This paper presents the main issues that must be considered to extend GPS to flexible systems. Sensor bandwidth, measurement accuracy, and receiver architecture issues are discussed as well as the techniques for real-time state estimation. This paper emphasizes the following:

1. *Why is GPS valuable as a structural deformation sensor?*
2. *What are the challenges to realizing this sensor?*
3. *How are these challenges being addressed?*

Introduction

GPS has traditionally been a navigation sensor for land, air, and sea vehicles. The system consists of 24 satellites, each of which broadcasts a signal (for general use) composed of three main parts: a 1.5 GHz carrier, a digital modulation sequence unique to each satellite, and a data message containing satellite time and position information. Traditional GPS receivers measure the range from the antenna to 4 or more satellites by observing the phase of the digital data sequence received from each satellite. These measurements enable a receiver to solve for its three dimensions of position plus the offset in the receiver's imperfect time estimate.

Basic GPS can locate a user within approximately 50 meters anywhere on the globe. A technique called differential GPS (DGPS) can locate a user to approximately 5 meters by using corrections broadcast from a local reference receiver of known position. More recently, techniques have been developed which make use of the GPS carrier. One such technique is called differential carrier phase (DCP), which relies on the measurement of the phase difference between two antennas receiving the same carrier signal. Assuming that the signal source is at an infinite distance, the incoming received wavefronts are planar. The quantity measured by the pair is the component of the vector between the antennas (the baseline vector) in the direction of the signal source (see Fig. 1). If the two antennas can be more than one carrier wavelength, λ, apart (about 19 cm), there is an unknown number of integer waves, η, which must be determined. The process of initially finding η is called integer ambiguity resolution. Once η is known, it can be tracked as long as the receiver

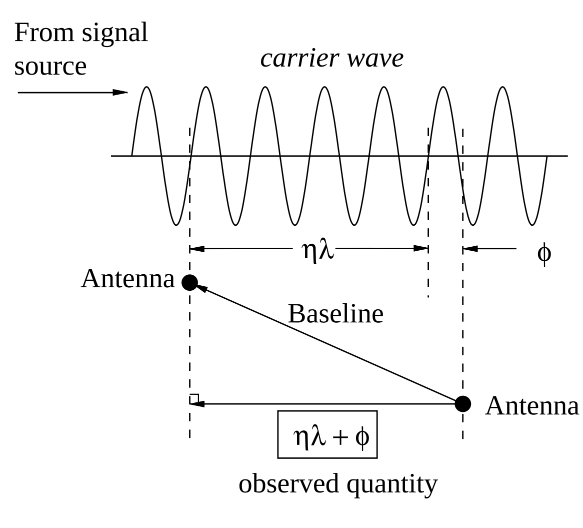

Figure 1: GPS Differential Carrier Phase Measurement

*Graduate research assistant, student member AIAA
†Assistant professor, Member AIAA
‡Graduate research assistant
§Professor, Fellow AIAA

maintains continuous lock on the signal.

DCP techniques have been shown to provide vehicle attitude information to 0.1 deg accuracy at 10 Hz [2]. This performance was achieved using Trimble Navigation's Vector GPS receiver. Integer ambiguity resolution was achieved by taking measurements as the GPS satellites traversed the sky. The non-linearity in the measurement equation provides additional observability which enables integer resolution. The same receiver with some software modifications has been used successfully as an attitude sensor on-board an orbiting spacecraft [3]. Also of interest is the work done at Stanford to measure attitude rate by measuring the rate of change of differential carrier phase [4]. A technique related to these studies was shown to provide modal information of a beam vibrating in one dimension [5]. The primary vibration modes and frequencies were observed from DCP measurements taken while the test beam freely vibrated. This work was of limited practical usefulness due to its 1D nature and the lack of generality in the estimator.

The goal of this research is to extend previous work by providing full three dimensional deformation information for feedback control of the rigid body motion and elastic vibrations of a structure. A conceptual diagram of a general elastic structure, upon which DCP measurements are being made, is shown in Fig. 2. With multiple antenna pairs and signal directions, plus a structural dynamic model, we will show how the general 3D deformation state of a flexible system can be reconstructed.

The rest of this paper will focus on answering the three questions stated in the abstract. We will: discuss pertinent issues related to GPS DCP sensing, present an estimation algorithm and describe a simulation which was used for its development, and present the experimental test setup which we are using to verify these concepts and methods.

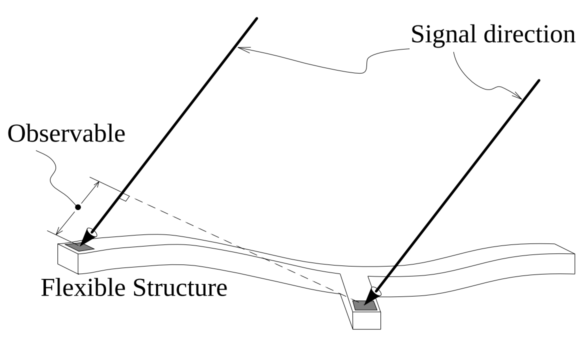

Figure 2: Observation for a Single Signal/Baseline Pair

GPS Issues

To answer the questions in the abstract, it is necessary to address several GPS sensor issues. First we consider the current bandwidth and noise limitations of GPS DCP sensing. GPS measures position (or relative position), and thus is not encumbered by the drifts observed with many rate or acceleration sensors. However, this good DC performance is offset by a current limitation in the achievable measurement bandwidth to approximately 5 Hz (Nyquist rate). Furthermore, since the carrier phase can be tracked to less than five percent of the total wavelength in typical signal to noise environments, the accuracy attainable once the integers have been resolved is on the order of a several millimeters over the receiver bandwidth. There are several space systems which have open loop modal frequencies and deflections in this range, such as solar panel arrays, flexible manipulator arms, and the main Space Station truss. GPS DCP can provide relative deflection information for alignment determination and control of the primary vibration modes of such systems.

Because GPS receiver design was originally based on the need for position fixes for ground and sea navigation, current receivers are not suited for rapid DCP output. As of this writing, there are no receivers on the market or in development known to the authors which take full advantage of the state of the art processor or data interface hardware. This is primarily because previous applications of GPS did not require the high performance hardware. However, plans to use GPS for attitude control of aircraft and spacecraft have brought attention to the need for higher bandwidth DCP sensing. It is anticipated that emerging technologies, such as the ones presented in this paper, will encourage development of receivers which take advantage of currently available, inexpensive, higher performance hardware.

Hardware changes may not be necessary to realize some significant improvements in DCP bandwidth and noise performance. A primary goal of this research is to push the frequency limit of carrier phase measurements on the current hardware. Recoding of the core programs is underway to streamline the measurement and output of DCP and to eliminate much of the code which has been developed for traditional applications, but is unnecessary for this end. For example, the current core code contains many routines specific to land and sea navigation which are not useful for this research, and which consume processing time. Any improvements will provide room for further optimization of tradeoffs between bandwidth and sensitivity.

If higher accuracy closed-loop control is required or higher frequency modes are of interest, the current GPS DCP system could be supplemented with a sensor with better high frequency response. This sensor would not be required to have good DC characteristics and thus might be simpler and less expensive than a stand-alone device.

Another important GPS issue is integer ambiguity resolution. Previous methods rely on the knowledge that the antennas are mounted on an essentially rigid body. Cohen has shown that flexible motion of a platform is observable in the case of aircraft wing flexure [6]. But this formulation assumed negligible flexure during integer estimation. In the next section, we present an extension of the technique which can be applied to systems that exhibit elastic deformations during estimation. The solution involves the use of a structural dynamic model plus data collected during vibrational motion of the structure to estimate the correct integer set.

Finally, a large number of antennas may be necessary to supply enough measurements for observability of a flexible system. The current DCP receivers multiplex signals from only four antennas (consisting of three slaves, each of which provide a DCP measurement with respect to the one master antenna). One way to increase the number of measurements is to use a single antenna as the master for phase comparisons on two receivers. The common signal provides a means of synchronizing the receiver's clocks. A seven antenna example is shown in Fig. 3. This idea could be easily extended to many more antennas by cascading receivers together in the same way.

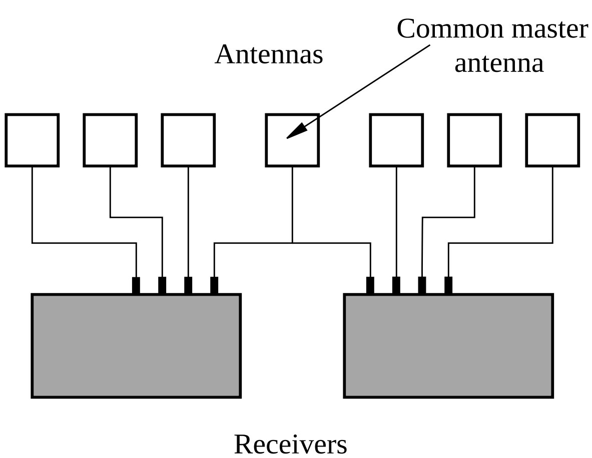

Figure 3: Seven Antenna Configurations

We are currently in the process of constructing a structure that can be used to investigate these various GPS sensing issues. Due to current bandwidth and sensitivity limitations of the GPS sensors, this structure has intentionally been make large so that it exhibits several very low frequency modes of vibration. Because this system is currently not operational, we verify the feasibility of using the GPS sensor on a simulation with analogous dimensions, frequencies, and noise characteristics. The next section illustrates how this simulation was used to develop the estimator for the system dynamics.

Dynamic State Estimation

Estimation of the state of the system of interest is challenging due to the non-linear measurement equation and the unknown integer component of each measurement. As discussed in the introduction, the GPS receiver has the ability to track the absolute carrier phase difference between two antennas, but it cannot determine the integer number of carrier waves in the measurement when carrier tracking is established. Thus an estimator is required.

A simplified model of an elastic structure was constructed to develop and test the estimator. This model has only two degrees of freedom, denoted by the angles q_1 and q_2 in Fig. 4. The base is inertially fixed, and all elements are rigid except the two beams, the members which connect the hubs. There is an antenna at the end of each of the rigid

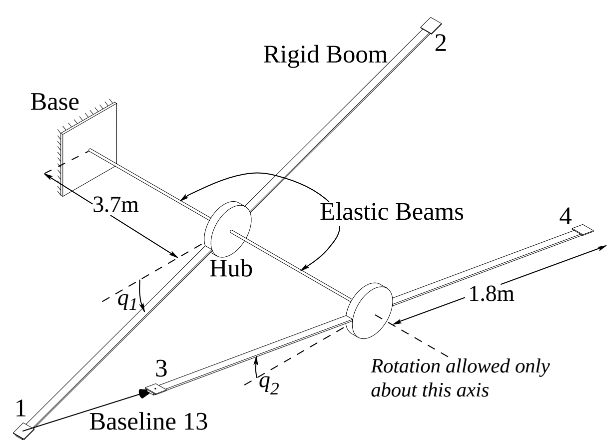

Figure 4: Simplified Dynamic System

booms. The four antenna locations are numbered on the figure. A baseline is a vector between any two antennas on the structure, and thus contains information about the deformation and orientation of the system. An example baseline vector is shown between sensors 1 and 3. The model is scaled in both size and vibration frequencies to closely match the real system which is discussed in the next section. Two modes are present with frequencies of 0.10 and 0.26 Hz.

With a master antenna and three slave antennas, three baseline vectors exist for this system. Four signal source directions were modeled, giving a total of 12 observables. The general DCP measurement equation for each observable is given by

$$\Delta\phi_{ij} = s_j^T b_i(x_k) - \lambda\eta_{ij} + \nu_{ij} \tag{1}$$

$i = 1, \ldots p, j = 1, \ldots r$, where,

p	number of baselines/slave antennas
r	number of satellites
m	$= p \cdot r$, number of measurements
λ	carrier wavelength
$\Delta\phi_{ij}$	difference in carrier phase from satellite j between antennas of baseline i, in meters ($0 \leq \Delta\phi_{ij} \leq \lambda$ at initial signal lock and unbounded thereafter)
s_j	unit line of sight vector to satellite j
b_i	ith baseline vector
η_{ij}	the integer component of baseline i/satellite j at initial signal lock
ν_{ij}	measurement noise

If the signal sources are at an infinite distance, the unit vectors, s_j, are the same for all antennas. The equations for one baseline, all satellites, may be stacked,

$$\Delta\phi_i = S^T b_i - \lambda\eta_i + \nu_i \tag{2}$$

where,

$$\Delta\phi_i = \begin{bmatrix} \Delta\phi_{i1} \\ \Delta\phi_{i2} \\ \vdots \\ \Delta\phi_{ir} \end{bmatrix}, \quad \eta_i = \begin{bmatrix} \eta_{i1} \\ \eta_{i2} \\ \vdots \\ \eta_{ir} \end{bmatrix}, \quad \nu_i = \begin{bmatrix} \nu_{i1} \\ \nu_{i2} \\ \vdots \\ \nu_{ir} \end{bmatrix},$$

$$S = \left[\; s_1 \; | \; s_2 \; | \cdots | \; s_r \; \right]$$

and stacked again for all baselines to form the overall matrix equation

$$\Delta\Phi = \begin{bmatrix} S^T b_1 \\ S^T b_2 \\ \vdots \\ S^T b_p \end{bmatrix} - \lambda\eta + \nu, \tag{3}$$

where,

$$\eta = \begin{bmatrix} \eta_1 \\ \eta_2 \\ \vdots \\ \eta_p \end{bmatrix}, \quad \nu = \begin{bmatrix} \nu_1 \\ \nu_2 \\ \vdots \\ \nu_p \end{bmatrix}$$

The GPS observation over time as a function of the system state is

$$y(x_k) = \Delta\Phi(x_k) + \lambda\eta \tag{4}$$

where x_k is the system state vector at time k. Thus, from (3) and (4), the standard measurement equation form is

$$y(x_k) = h_k(x_k) + \nu_k \tag{5}$$

$$h_k(x_k) = \begin{bmatrix} S^T b_1(x_k) \\ S^T b_2(x_k) \\ \vdots \\ S^T b_p(x_k) \end{bmatrix} \tag{6}$$

The state vector is composed of the four dynamic states q_1, $\dot{q}_1$, q_2, and $\dot{q}_2$, and is augmented with the m initial measurement integers

$$x_k = \begin{bmatrix} q_k \\ \eta \end{bmatrix} \begin{matrix} \}4 \\ \}m \end{matrix} \tag{7}$$

where,

$$q_k = \begin{bmatrix} q_1 \\ \dot{q}_1 \\ q_2 \\ \dot{q}_2 \end{bmatrix}_k$$

The discrete plant dynamics are described by

$$x_{k+1} = Ax_k + Bw_k \tag{8}$$

where w_k is process noise.

A simulation of the system dynamics was computed and sampled with a 0.12 second sampling interval. Process noise was added in the form of 0.02 rad/sec^2 standard deviation white gaussian angular accelerations of the two rigid sections, $\ddot{q}_1$ and $\ddot{q}_2$, applied at each sampling instance. Also, the GPS signal environment was simulated with added white gaussian measurement noise with a 1 cm standard deviation. This is a realistic noise magnitude in most signal/noise environments [1–3]. The system was simulated for both large and small angle free vibrations to test the non-linear performance and the sensitivity performance. A fully linearized estimator is possible for small angle motion for the simplified model. However, the non-linear form was retained to handle the likely large angle motion (including rigid body motion) of the actual test structure.

An Extended Kalman Filter (EKF) was implemented and was found never to converge to the correct state (for the large angles simulation) given a random initial guess and large initial covariance matrix. A method was developed to provide initial state and covariance matrix estimates to start the EKF. A batch non-linear least squares estimate of the state was performed on a fraction of the initial data assuming no process noise. The batch algorithm proceeds as follows:

1. A guess of the initial state is propagated using the model, neglecting process noise.
2. The measurement equation is linearized at each sample in the data set about the current estimate.
3. A linear least squares problem is solved for a change in the initial state.
4. Iterate until a convergence criteria is reached.

The batch estimate was iterated until the integer state residuals had converged to a prescribed limit, usually bringing the integers within 1-2 of their correct values. Very few data points had to be included in the batch fit to insure convergence, in fact only 20 points (2.4 seconds) of data were used for the trials presented here. This is an encouraging result because the computational effort required for the batch estimation grows $\sim n^3$, where n is the number of states.

The EKF algorithm is the standard form of an estimator for discrete time systems with non-linear measurements [8]. During each iteration, there is a time update and a measurement update. Quantities after time update are denoted by an over-bar ($\bar{\ }$), and after measurement update by a hat ($\hat{\ }$). E denotes the expectation operator.

The white measurement noise and process noise covariances are, respectively,

$$V = E[\nu_k \nu_k^T], \qquad W = E[w_k w_k^T]$$

Time update:

$$\bar{x}_k = A\hat{x}_{k-1} \tag{9}$$

$$\bar{P}_k = A\hat{P}_{k-1}A^T + BWB^T \tag{10}$$

Measurement update:

$$K_k = \bar{P}_k H_k^T [V + H_k \bar{P}_k H_k^T]^{-1} \tag{11}$$

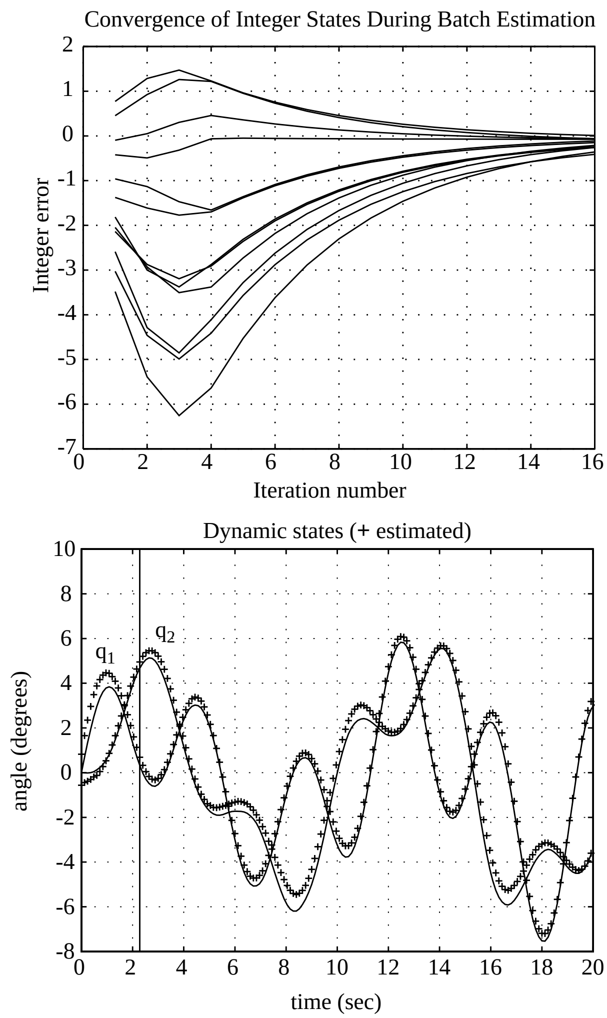

Figure 5: Results of Batch/Recursive Estimator for Baseline13

$$\hat{P}_k = [I - K_k H_k]\bar{P}_k \tag{12}$$

$$\hat{x}_k = \bar{x}_k + K_k[y_k - h_k(\bar{x}_k)] \tag{13}$$

where,

$$H_k = \left.\frac{\partial h_k(x_k)}{\partial x_k}\right|_{x_k = \bar{x}_k}$$

and h_k may be differentiated analytically from Eq. 6.

The batch estimator gives an initial state (including the constant integers) and initial covariance matrix from which the recursive (and computationally efficient) EKF is propagated. The following plots illustrate the results of the simulation for relatively small angle motion. The results for large angle motion are similar. Fig. 5 shows the integer convergence during the batch estimation and shows the results of the EKF using initial conditions provided by the

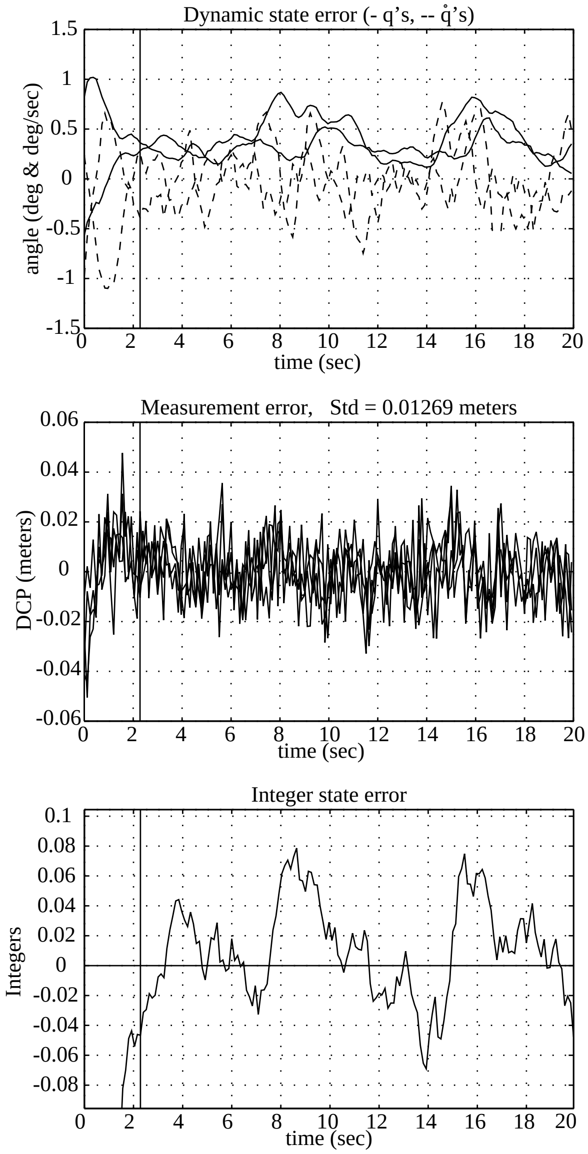

Figure 6: Results of Batch/Recursive Estimator for Baseline13

batch. The data from t=0 to the vertical line (at about 2 seconds) was processed in the batch estimation. Fig. 6 shows the state error, as well as the measurement error, and an example integer state of the Baseline13 shown in Fig. 4. The estimator converged to within 0.3 deg degrees RMS of the q_1 and q_2 states.

There are many parameters to choose when using this algorithm. For instance, we must address:

1. *How much data should be used in the batch estimation process?*
2. *How far should the batch be allowed to converge and what is the convergence criterion?*
3. *Should the integers be retained in the state after integer convergence?*

The amount of data used is a tradeoff between computational speed and observability of the system dynamics. Also, since no process noise was assumed in the batch estimation, a shorter block of data is advantageous. It was observed that using very large blocks of data did not greatly reduce the number of iterations to convergence, but did greatly increase the computation time per iteration. The measurement residual vector magnitude was used as the stopping criteria for this simulation.

After the EKF had been properly tuned, it was found to converge readily for relatively coarse initial conditions (integers within about 10). Tuning involved prescribing a fictitious amount of integer state process noise covariance (in the W matrix) to prevent the filter gains associated with the integer states from going to zero. The initial covariance estimate appears to be more important than the initial state estimate for convergence. In fact, reliable convergence was observed with a good covariance estimate but a random choice of state initial condition. The robustness of this method is encouraging, but for applications requiring high integrity, allowing the batch to converge all the way to the correct integer set could be more desirable. Once the integers are known, they will change only in the event of a cycle slip in the receiver phase lock loop, or if a signal is lost then re-acquired. Thus the integers could be dropped from the state in the EKF, resulting in a much smaller estimator. However, leaving integers in the state would enable relatively seamless cycle-slip detection and correction.

A proposed flow algorithm for the real-time estimator is shown in Fig. 7. When the batch estimator is activated, it processes the data and reports an initial state and covariance to the EKF. The buffer holds data from a specified amount of time in the past to the current time. The EKF runs and outputs state estimates until it detects a convergence failure. Such a failure could be due to a cycle slip or a lost signal. The EKF is then re-initialized by a new batch estimate.

Further refinements of the estimation algorithm will be necessary to account for lost and re-acquired signals. Also, the robustness of the estimator to non-white process and measurement noise, as well as

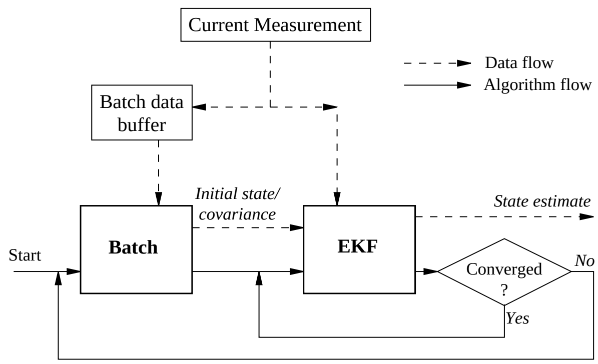

Figure 7: Estimation Algorithm

model error, will be investigated.

Test Facility

A ground testing facility has been constructed to verify this developed theory. Tests are being performed on a 30 foot long, 500 pound vertically suspended elastic assembly designed to move in a way analogous to a free flying space structure, exhibiting large deflections and slow vibrations in three dimensions. Slow motions and large deflections are needed due to the current bandwidth and sensitivity of the GPS DCP sensor. The structure consists of three 10 inch cubed solid aluminum blocks which are connected together with thin-wall aluminum tubing (see Fig. 8). Each block is suspended vertically by a thin, 40 foot cable which attaches very near the center of mass of the block. This allows nearly free rotation of each block about it's own center of mass, thus imitating the motion of a freely floating structure. Preliminary tests of the assembly confirm that the first bending mode vibration frequency is 0.15 Hz and first twist mode 0.21 Hz. This shows the primary vibrations modes of the test structure to be well within the measurable bandwidth of the GPS DCP sensor. A photograph of the test structure is shown in Fig. 9. The picture shows the three main structural blocks resting on tables, connected by the elastic beams. The GPS antennas are visible at the ends of each of the booms.

The entire assembly is hung from a bearing which allows free rotation of the structure about a vertical axis. This provides an rigid body degree of freedom. The suspension cables are as long as feasible to reduce the frequency of suspension induced pendulum modes. Although the dynamics are not exactly what would be expected on orbit, this design exhibits many of the vibration characteristics necessary to allow testing and verification of the GPS system. This test-bed is an extension of previous work on a system which had only one degree freedom [5]. The addition of axial rotation and the rigid body degrees of freedom allow development and testing of estimators and controllers applicable to more realistic systems.

To emulate the GPS signal environment indoors, eight pseudolite GPS transmitters have been built following the work of Cobb [7] and Zimmerman [10]. The pseudolites are mounted on all sides of the testing room to provide signals for measurement at the structure. The experimental room is very large (approx. 200 x 100 x 60 ft) allowing the signal sources to be sufficiently distant from the structure and it's antennas. This allows the assumption that the line of sight vectors and signal strengths are the same at all antennas. A picture of the experimental hardware is shown in Fig. 10. The palm-sized pseudolite can operate on a standard 9 volt battery. Both the pseudolite and the helical transmit antenna were designed and manufactured here at Stanford. The transmitting hardware is mounted on the walls of the testing room, and the receiving hardware is on the testing structure.

A dynamic model of the test structure has been obtained by modeling each elastic beam as a sequence of rigid elements connected by rotational springs and dampers. The resulting model, including all suspension system effects has been linearized, simulated and animated using three-dimensional com-

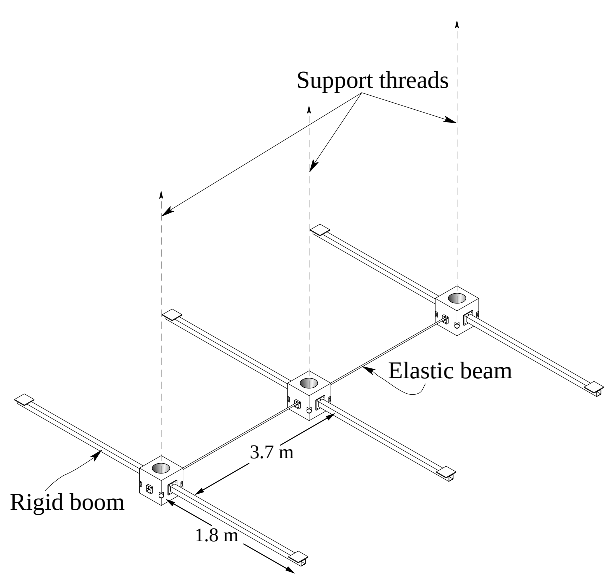

Figure 8: Test Structure

Figure 9: Photograph of Test Assembly

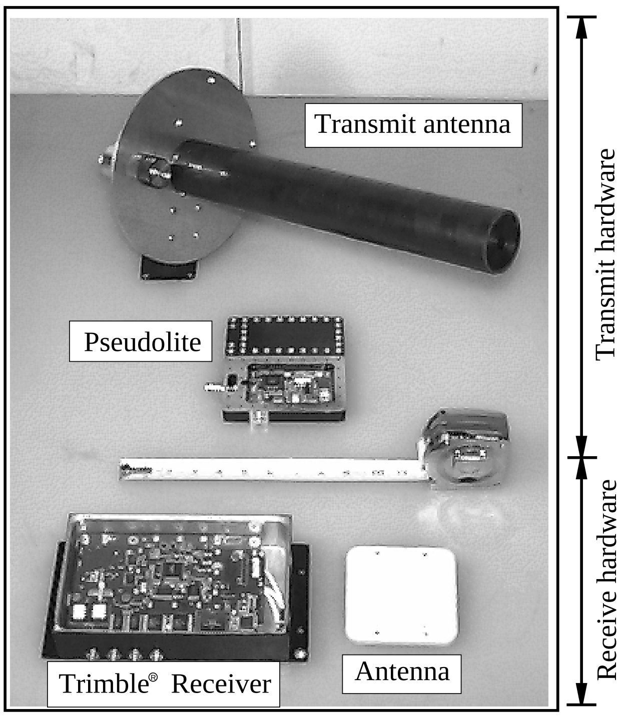

Figure 10: GPS Hardware

puter graphics software. This provides a convenient means of visualizing the structural motion especially when under the influence of feedback control actuation. Several actuator schemes are under investigation, but due to the size of the structure, the most feasible is probably based on an array of cold gas thrusters, similar to the system used for control of robot motion in the Stanford Aerospace Robotics Lab [9].

Conclusions

Based on the issues and methods discussed, GPS has been shown to be a viable and valuable structural deformation sensor for systems which exhibit vibrations with centimeter level deflections up to approximately a 2 Hz bandwidth. The excellent low frequency performance of the GPS DCP system due to its direct position sensing makes it ideal for measurement and control of the primary vibration modes of such flexible systems. Also, it is anticipated that bandwidth and sensitivity of receivers may be improved by taking advantage of advances in solid-state electronics technology.

To test this system, an experiment is under construction consisting of a large, flexible structure and electronic equipment to emulate the GPS signal environment indoors. The structure has motions which are detectable and in the bandwidth of the sensor. A simplified system which captures the primary characteristics important for analyzing the GPS DCP sensor, and has physical size and vibrations frequencies similar to the real structure, was simulated. Based on the excellent performance of the estimator algorithms presented, these simulations strongly suggest that the techniques shown will extend to the actual test system and provide state estimates for real-time feedback control.

References

[1] C. E. Cohen and B. W. Parkinson, "Expanding the Performance Envelope of GPS-Based Attitude Determination," in *Proc. Institute of Navigation ION-GPS 91,* Albuquerque, NM, 1991.

[2] C. E. Cohen and B. W. Parkinson, "Aircraft Applications of GPS-based Attitude Determination," in *Proc. Institute of Navigation ION-GPS 92,* Albuquerque, NM, 1992.

[3] C. E. Cohen, E. G. Lightsey, B. W. Parkinson, W. A. Feess, "Space Flight Tests of Attitude Determination Using GPS," in *Proc. Institute of Navigation ION GPS-93,* Salt Lake City, Utah, 1993.

[4] P. Y. Montgomery, H. Uematsu, B. W. Parkinson, "Analysis of Angular Velocity Determination Using GPS." in *Proc. Institute of Navigation ION GPS-94,* Salt Lake City, Utah, 1994.

[5] Harris Teague and Bradford W. Parkinson, "Translation, Rotation, and Vibration Control of Large Space Structures Using Self-Differential GPS (SDGPS)," Guidance and Control 1993, Vol. 81, Advances in the Astronautical Sciences. American Astronautical Society, 1993.

[6] C. E. Cohen, *Attitude Determination Using GPS,* Ph.D. Dissertation, Stanford University, 1993.

[7] H. S. Cobb, C. E. Cohen, B. W. Parkinson, "Theory and Design of Pseudolites," in *Proc. Institute of Navigation National Technical Meeting,* San Diego, CA, 1994.

[8] Gelb, A., ed. *Applied Optimal Estimation,* M.I.T Press, 1974.

[9] M. A. Ullman, *Experiments in Autonomous Navigation and Control of Multi-manipulator, Free-flying Space Robots,* Ph.D. Dissertation, Stanford University, SUDAAR 630, 1993.

[10] K. R. Zimmerman, R. H. Cannon, Jr, "Differential Carrier Phase GPS Techniques for Space Vehicle Rendezvous," in *Proc. Institute of Navigation ION GPS-94,* Salt Lake City, Utah, 1994.